ON THE COMPARISON OF TWO ROOM COMPENSATION / DEREVERBERATION METHODS EMPLOYING ACTIVE ACOUSTIC BOUNDARY ABSORPTION

Jacob Donley[⋆]*, Christian Ritz*[⋆] *and W. Bastiaan Kleijn*[†]

[⋆] School of Electrical, Computer and Telecommunications Engineering, University of Wollongong, Australia
[†] School of Engineering and Computer Science, Victoria University of Wellington, New Zealand

ABSTRACT

In this paper, we compare the performance of two active dereverberation techniques using a planar array of microphones and loudspeakers. The two techniques are based on a solution to the Kirchhoff-Helmholtz Integral Equation (KHIE). We adapt a Wave Field Synthesis (WFS) based method to the application of real-time 3D dereverberation by using a low-latency pre-filter design. The use of First-Order Differential (FOD) models is also proposed as an alternative method to the use of monopoles with WFS and which does not assume knowledge of the room geometry or primary sources. The two methods are compared by observing the suppression of reflections off a single active wall over the volume of a room in the time and (temporal) frequency domain. The FOD method provides better suppression of reflections than the WFS based method but at the expense of using higher order models. The equivalent absorption coefficients are comparable to passive fibre panel absorbers.

Index Terms— active acoustic absorption, active noise control (ANC), active room compensation, dereverberation, wave field synthesis (WFS).

1. INTRODUCTION

The active control of acoustic sound fields is a useful process for suppressing undesirable sound over large spaces. Acoustic reflections, or echoes, inside listening rooms are a common source of undesirable sound field contributions, notably, in the degradation of sound field reproductions using Wave Field Synthesis (WFS) [1] or Higher Order Ambisonics (HOA) [1], [2]. Active Noise Control (ANC) [3] is a method that allows for real-time cancellation of sound and there exist room equalisation and dereverberation techniques [4]–[6] to reduce the influence of reflections on system performance.

While the majority of dereverberation techniques focus on post-processing the recorded signals [7]–[9] there has been research into the real-time suppression of reflected sound fields [5], [10], [11]. The suppression of any sound field requires synthesis of a desired sound field and is commonly called Sound Field Synthesis (SFS) [1]. Some SFS methods use higher-order loudspeakers and/or microphones to reduce error or loudspeaker counts [12]–[14]. While there are numerous techniques to perform SFS, the state-of-the-art methods generally rely on a solution to the wave equation [15], often with the Kirchhoff-Helmholtz Integral Equation (KHIE) [1], [2], [16]. The KHIE states that complete knowledge of a sound field boundary is sufficient knowledge to determine the sound field in the bounded space [15]. While the KHIE is defined for enclosed boundaries, some systems work for partial boundaries by secondary source selection or using specially designed aperture functions [15]–[17].

Dedicated calibration processes often used to compensate for reverberation in listening rooms [18], [19] require knowledge of the room, or the room itself, and provide compensation tailored to the particular room. Other techniques employ pre-filtering of single loudspeaker channels by reshaping Room Impulse Responses (RIRs) [7], [8]. Further approaches rely on feedback from microphones within the cancellation region to adapt filters using Wave-Domain Adaptive Filtering (WDAF) or modal decompositions [5], [10], [11].

ANC systems generally rely on a feedforward or feedback system which require error microphones to adaptively weight the system and reduce errors from its previous state [3], [20]. While the adaptive nature of ANC systems generally ensure convergence to an optimal solution, the convergence rate may be slow and any abrupt changes in the environment may degrade performance [3]. These systems often require modelling of secondary paths between the secondary sources and the error microphones. Improvement of the erroneous secondary path models is a topic of ongoing research. There exist ANC techniques which do not require secondary path modelling but their convergence rate is lower than state-of-the-art ANC techniques, such as the Filtered-x Least Mean Square (FxLMS) algorithm [21]–[24]. Other methods remove filtering delay by using autoregressive models [17] and use reflections to aid cancellation [25].

While the majority of ANC algorithms rely on single or multi-point approaches some applications rely on ANC over larger areas, such as the cancellation of vehicle cabin noise or sound across barriers [17], [26], [27]. The recording and reproduction of a sound field over a large space, termed Wave Field Reconstruction (WFR), has been thoroughly researched [28], [29] and real-time systems have been realised [30]. The inherent latency, when using current filter designs, of real-time WFR systems deems them unusable for applications of non-adaptive ANC. Low-latency, or zero-latency, WFR filters are required for non-adaptive and/or low-latency ANC.

In this work, we consider dereverberation in closed rooms by absorbing reflections using an active wall. We look at two possible methods; the first is using monopole models with a WFS-based method and the second is using differential (pressure gradient) models as a direct solution to the KHIE. For the first technique we provide a novel contribution by repurposing the WFR method for 3D boundary cancellations and reducing the need for adaptive filters. We propose the use of a Weighted Least-Squares (WLS) pre-filter for low-latency reproduction and cancellation. For the second method we propose the use of FOD (pressure gradient) models as implicit solutions to the KHIE or WFS/WFR pre-filter problem.

A description of the KHIE is given in section 2 and the WFR derivation in section 3. The proposed WLS pre-filter design is described in section 4 and the FOD models method is given in section 5. Results, discussion and conclusions are given in sections 6 and 7.

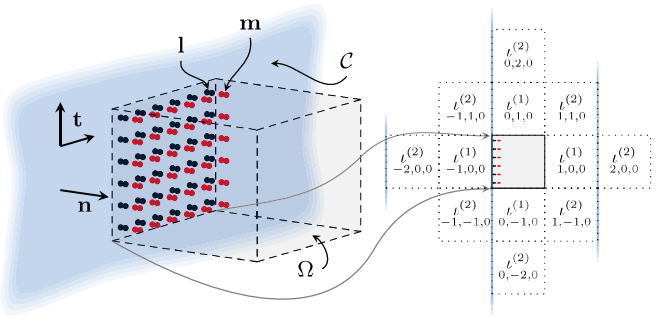

Fig. 1: An active dereverberation scenario is shown. Left: Active dipole wall (black loudspeakers and red microphones) and spatial 3D geometry. Right: Equivalent image source layout for the evaluation.

1.1. Notations and Definitions

In this work, we assume 3D Cartesian coordinate space with no specific origin. The volume enclosed by the room is denoted as Ω with the room boundary of interest, $\mathcal{C} \equiv \partial\Omega$, and observation points are $\mathbf{x} \in \Omega$. Loudspeaker locations are $\mathbf{l}$ and microphone locations are $\mathbf{m}$. The normal to $\mathcal{C}$ is $\mathbf{n}$ and the tangential plane, $\mathbf{t}$, is perpendicular to $\mathbf{n}$. The wavenumber is $k = \omega/c$ where ω is the angular frequency and $c = 343\,\mathrm{m\,s^{-1}}$ is the speed of sound in air. The unit imaginary number is $i = \sqrt{-1}$. The image source notation in Fig. 1 is given as $\iota^{(\bar{n})}_{x,y,z}$ where $\bar{n}$ is the order of the image source and (x, y, z) are the coordinates of the imaged room relative to the primary room.

2. KIRCHHOFF-HELMHOLTZ INTEGRAL EQUATION

The KHIE provides a solution to the homogeneous wave equation. The Greens function, $G(\mathbf{x}, \mathbf{x}'; \omega) : \Omega \times \mathbb{R} \to \mathbb{C}$, is given in three dimensional coordinate space, $\Omega \subset \mathbb{R}^3$. The KHIE is given by [15]

$$\boldsymbol{\Phi}(\mathbf{x};\omega) = \iint_{\mathcal{C}} G(\mathbf{x}, \mathbf{x}_0; \omega) \underbrace{\frac{\partial \boldsymbol{\Phi}(\mathbf{x}_0;\omega)}{\partial \mathbf{n}}}_{\dot{Q}(\mathbf{x}_0;\omega)} - \underbrace{\boldsymbol{\Phi}(\mathbf{x}_0;\omega)}_{\ddot{Q}(\mathbf{x}_0;\omega)} \frac{\partial G(\mathbf{x}, \mathbf{x}_0;\omega)}{\partial \mathbf{n}}\, d\mathcal{C} \quad (1)$$

$\mathbf{x}_0 \in \mathcal{C}$, where $\boldsymbol{\Phi}(\mathbf{x};\omega)$ is an any solution to (1) and the monopole and dipole driving signals are $\dot{Q}(\mathbf{x}_0;\omega)$ and $\ddot{Q}(\mathbf{x}_0;\omega)$, respectively.

The KHIE, as it is given in (1), is over-specified [15] and can be simplified by using the Neumann Green function, $G_{\mathcal{N}}(\mathbf{x}, \mathbf{x}_0; \omega)$, for monopoles as is done for WFS and the Spectral Division Method (SDM). The simplified KHIE for monopoles is

$$\boldsymbol{\Phi}(\mathbf{x};\omega) = \iint_{\mathcal{C}} G_{\mathcal{N}}(\mathbf{x}, \mathbf{x}_0; \omega) \frac{\partial \boldsymbol{\Phi}(\mathbf{x}_0;\omega)}{\partial \mathbf{n}}\, d\mathcal{C} \quad (2)$$

$$= \iint_{\mathcal{C}} \underbrace{-2\frac{\partial \boldsymbol{\Phi}(\mathbf{x}_0;\omega)}{\partial \mathbf{n}}}_{Q_{\mathrm{WFS}}(\mathbf{x}_0;\omega)} G(\mathbf{x}, \mathbf{x}_0;\omega)\, d\mathcal{C} \quad (3)$$

where $Q_{\mathrm{WFS}}(\mathbf{x}_0;\omega)$ is the WFS loudspeaker driving signal [28].

3. WAVE FIELD RECONSTRUCTION (WFR)

Previous work has shown that the WFS method can be used to accurately reproduce sound fields from sound field recordings [28]. Recently, the WFR filtering method has looked at efficiently transforming recorded signals into driving signals [29], [30]. In this section we propose a method for the design and use of a WFR filter for low-latency real-time dereverberation.

3.1. Receiving

We start by defining a desired sound field, $S^{\mathrm{d}}(\mathbf{x};\omega) \equiv \boldsymbol{\Phi}(\mathbf{x};\omega)$, reflected by a boundary wall and which is to be cancelled. A planar monopole microphone and loudspeaker array are placed at the boundary. The planar microphone array and secondary source loudspeaker array are both modelled as continuously distributed arrays.

The sound pressure gradient at the microphone array is used to find the reflected sound field back in to the room. The reflections are the half-space sound field of the loudspeaker wall.

The Rayleigh I integral from (3) gives the desired 3D spatio-temporal sound field [29]

$$S^{\mathrm{d}}(\mathbf{x};\omega) = -2 \iint_{\mathcal{C}} \frac{\partial S^{\mathrm{d}}(\mathbf{m};\omega)}{\partial \mathbf{n}} G(\mathbf{x}, \mathbf{m};\omega)\, d\mathcal{C},\ \forall \mathbf{m} \in \mathcal{C}, \quad (4)$$

where $\partial/\partial\mathbf{n}$ is the pressure gradient at $\mathcal{C}$, the noiseless desired sound pressure at the microphones, $\mathbf{m} \equiv \mathbf{x}_0$, is $S^{\mathrm{d}}(\mathbf{m}; k)$ and, for half-space and small $\|\mathbf{m} - \mathbf{l}\|$, we assume the free space Greens function [15],

$$G(\mathbf{x}, \mathbf{x}';\omega) = \frac{e^{i\frac{\omega}{c}\|\mathbf{x}-\mathbf{x}'\|}}{4\pi\|\mathbf{x}-\mathbf{x}'\|}. \quad (5)$$

The goal now is to find the relationship between the microphone signals and the desired loudspeaker signals by using $S^{\mathrm{d}}(\mathbf{x};\omega)$.

3.2. Reproduction

The actually reproduced sound field, $S^{\mathrm{a}}(\mathbf{x};\omega)$, of the planar loudspeaker array is given by [15],

$$S^{\mathrm{a}}(\mathbf{x};\omega) = \iint_{\mathcal{C}} Q_{\mathrm{WFS}}(\mathbf{l};\omega) G(\mathbf{x}, \mathbf{l};\omega)\, d\mathcal{C},\ \forall \mathbf{l} \in \mathcal{C}. \quad (6)$$

The reproduced sound field, $S^{\mathrm{a}}(\mathbf{x};\omega)$, must match that of the inverted reflected sound field, $-S^{\mathrm{d}}(\mathbf{x};\omega)$, so that $S^{\mathrm{a}}(\mathbf{x};\omega) = -S^{\mathrm{d}}(\mathbf{x};\omega)$. The loudspeaker array and microphone array share the boundary, $\mathcal{C}$, where $\mathbf{l} \equiv \mathbf{m}$, and so (3) and (4) give

$$Q_{\mathrm{WFS}}(\mathbf{l};\omega) = 2\frac{\partial S^{\mathrm{d}}(\mathbf{m};\omega)}{\partial \mathbf{n}}, \quad (7)$$

where the sound pressure gradient at $\mathbf{m}$ is found using Euler's equation as (a tilde indicating the spatial frequency domain) [29]

$$\frac{\partial S^{\mathrm{d}}(\mathbf{m};\omega)}{\partial \mathbf{n}} = \frac{\partial}{\partial \mathbf{n}} \left(\frac{1}{4\pi^2} \iint_{\mathcal{C}} \widetilde{S}^{\mathrm{d}}(k_{\mathbf{t}};\omega) e^{-ik\mathbf{x}}\, dk_{\mathbf{t}} \right) \quad (8)$$

$$= \frac{1}{4\pi^2} \iint_{\mathcal{C}} -ik_{\mathbf{n}} \widetilde{S}^{\mathrm{d}}(k_{\mathbf{t}};\omega) e^{-ik_{\mathbf{t}}\mathbf{t}}\, dk_{\mathbf{t}} \quad (9)$$

$$= -ik_{\mathbf{n}} S^{\mathrm{d}}(\mathbf{m};\omega) \quad (10)$$

and $k_{\mathbf{n}} = \sqrt{k^2 - k_{\mathbf{t}}^2}$. The loudspeaker driving signal is then

$$Q_{\mathrm{WFS}}(\mathbf{l};\omega) = F(e^{ik}) S^{\mathrm{d}}(\mathbf{m};\omega), \quad (11)$$

$$F(e^{ik}) = -2ik_{\mathbf{n}}. \tag{12}$$

The desired loudspeaker signals are given by the microphone signals with the parameter-independent multiplier operator, $F(e^{ik})$.

4. PLANAR ARRAY WFS/SDM PRE-FILTER DESIGN

The relationship between sound pressure and particle velocity gives rise to a $+6\,\mathrm{dB/oct}$ magnitude gain with a constant 90° phase shift. The section describes the design of a filter required to compensate for $F(e^{ik})$ so that the reproduced sound field is of the correct amplitude and phase for cancellation to occur.

4.1. Weighted Least Squares (WLS) Method

While it is simple to create a linear-phase Finite Impulse Response (FIR) filter directly from $F(e^{ik})$ which provides $+6\,\mathrm{dB/oct.}$ gain and 90° phase shift, it is not as simple to design a minimum-phase equivalent. Linear-phase is suitable for applications which do not require low-latency filtering, such as for the reproduction of a pre-recorded sound field. However, for sound field cancellation, low-latency and filter accuracy is important. The WLS method can approximate the desired response while the weighting relieves constraint on the minimisation for frequency bands that are of less importance.

The WLS compensation filter

$$H(z) \triangleq \frac{B(z)}{A(z)} \triangleq \frac{\sum_{m=0}^{N_b} b_m z^{-m}}{\sum_{m=0}^{N_a} a_m z^{-m}}, \tag{13}$$

can be found by minimising the error

$$\min_{b_m, a_m} \sum_{m=0}^{\widehat{N}} \left| \left(A(e^{ik_m}) F(e^{ik_m}) - B(e^{ik_m}) \right) W(k_m) \right|^2, \tag{14}$$

where $\widehat{N} = N - 1$, discrete Fourier transform (DFT) length is N and $W(k_m)$ is a bandpass weighting for $F(e^{ik})$.

The WLS approach is implemented with

$$\begin{bmatrix} \mathbf{B} \\ \mathbf{A} \end{bmatrix} = (\mathbf{D}^H \mathbf{W} \mathbf{D})^{-1} \mathbf{D}^H \mathbf{W} \mathbf{f}, \tag{15}$$

where $\{\cdot\}^H$ denotes a Hermitian transpose,

$$\mathbf{D} = \begin{bmatrix} -1 & \cdots & -1 \\ -e^{-i\pi k_0/\hat{k}} & \cdots & -e^{-i\pi k_{\widehat{N}}/\hat{k}} \\ \vdots & \ddots & \vdots \\ -e^{-N_b i\pi k_0/\hat{k}} & \cdots & -e^{-N_b i\pi k_{\widehat{N}}/\hat{k}} \\ F(e^{ik_0}) e^{-i\pi k_0/\hat{k}} & \cdots & F(e^{ik_{\widehat{N}}}) e^{-i\pi k_{\widehat{N}}/\hat{k}} \\ \vdots & \ddots & \vdots \\ F(e^{ik_0}) e^{-N_a i\pi k_0/\hat{k}} & \cdots & F(e^{ik_{\widehat{N}}}) e^{-N_a i\pi k_{\widehat{N}}/\hat{k}} \end{bmatrix}^T, \tag{16}$$

$$\mathbf{W} = \mathrm{diag}\left(\begin{bmatrix} W(k_0) & \cdots & W(k_{\widehat{N}}) \end{bmatrix} \right), \tag{17}$$

$$\mathbf{f} = -\begin{bmatrix} F(e^{ik_0}) & \cdots & F(e^{ik_{\widehat{N}}}) \end{bmatrix}^T \tag{18}$$

and $\hat{k} = 2\pi f_\mathrm{s}/c$ with sampling frequency, f_s. The WLS solution gives the coefficients

$$\mathbf{B} = \begin{bmatrix} b_0 & \cdots & b_{N_b} \end{bmatrix}^T, \qquad \mathbf{A} = \begin{bmatrix} a_0 & \cdots & a_{N_a} \end{bmatrix}^T, \tag{19}$$

which are used to construct the desired filter, $H(z)$, using (13). The weight can then be designed to relieve the constraint on the least squares optimisation as described in the following section.

4.2. Weight Design

Due to the discretised loudspeaker and microphone array, there is an aliasing frequency, k_u, where accuracy degrades at higher frequencies. In practice it is unnecessary to constrain the filter design above k_u.

The value of k_u is dependent on the finite spacing between array elements. Its lowest value is used to find the least squares weighting

$$W(k) = \begin{cases} 1, & k \le k_\mathrm{u} \\ 0, & k > k_\mathrm{u} \end{cases}, \qquad k_\mathrm{u} = \frac{\pi}{\Delta \mathbf{l}} = \frac{\pi}{\Delta \mathbf{m}}, \tag{20}$$

where $\Delta\mathbf{l}$ and $\Delta\mathbf{m}$ are the spacing between adjacent loudspeakers and microphones, respectively, and $W(k)$ weights the importance of the minimisation above and below k_u. Other weights may give low-latency low-pass filters thus reducing the influence of aliasing.

5. HALF-SPACE RECORDING AND REPRODUCTION

In practice, it is important for the microphone wall to record only the signal coming from the half-space within the room and, similarly, for the loudspeaker wall to only reproduce into the half-space that is the room. While omnidirectional monopole models simplify the analysis of the problem, their implementation in practice is less desirable than FOD models which can be less dependent on feedback loops. In this section, an overview of the FOD model used in this work is given.

5.1. First-Order Differential (FOD) Source/Receiver Model

As can be seen from (12), the multiplier operator has most influence along the normal, $\mathbf{n}$. However, the filter designed using (13) and (15) is spatially independent and, therefore, does not approximate the response of $F(e^{ik})$ along the plane, $\mathbf{t}$. This results in inaccurate cancellation for sound components propagating parallel to $\mathbf{t}$.

FOD receivers and sources are better suited to the KHIE as they are, themselves, a combination of monopole and dipole responses. Measuring the pressure and particle velocity on $\mathcal{C}$ allows for the driving signals to be directly obtained. Using (1) we have

$$S^\mathrm{a}(\mathbf{x};\omega) = \iint_\mathcal{C} G(\mathbf{x},\mathbf{l};\omega)\, \dot{Q}(\mathbf{l};\omega) - \ddot{Q}(\mathbf{l};\omega) \frac{\partial G(\mathbf{x},\mathbf{l};\omega)}{\partial \mathbf{n}}\, d\mathcal{C}, \tag{21}$$

$$\dot{Q}(\mathbf{l};\omega) = -\frac{\partial S^\mathrm{d}(\mathbf{m};\omega)}{\partial \mathbf{n}}, \qquad \ddot{Q}(\mathbf{l};\omega) = -S^\mathrm{d}(\mathbf{m};\omega), \tag{22}$$

resulting in the monopole and dipole driving signals being directly obtained from the dipole and monopole microphone signals, respectively. The ratio of $|\dot{Q}(\mathbf{l};\omega)|$ to $|\ddot{Q}(\mathbf{l};\omega)|$ gives the *time delay ratio* which can be used to determine the radiation pattern of the FOD model for small dipole separation distances.

6. RESULTS AND DISCUSSION

6.1. Experimental Setup

For the evaluations, a cube shaped room is used with 3 m length sides and a single wall consists of a planar microphone and loudspeaker array as depicted in Fig. 1. Both microphone and loudspeaker arrays consist of a 60×60 grid of receivers and sources, respectively. The microphone and loudspeaker spacings are $\Delta\mathbf{m} = \Delta\mathbf{l} = 5\,\mathrm{cm}$ and the aliasing frequency is $k_\mathrm{u} = 2\pi(3.43\,\mathrm{kHz})/(343\,\mathrm{m\,s^{-1}})$. The sampling frequency is $f_\mathrm{s} = 48\,\mathrm{kHz}$ and DFT length $N = 4096$ with $N_b = 4$ and $N_a = 1$. The order of reflections is set to $\bar{n} = 2$ for

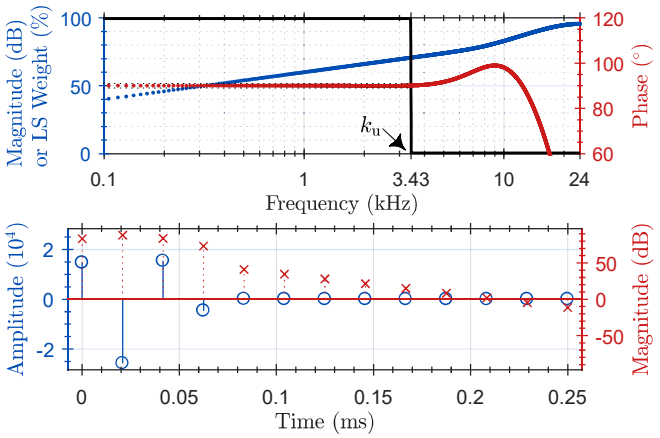

Fig. 2: Low-latency WFR WLS filter frequency response (top) and impulse response (bottom) are shown. The LS weight shown in black.

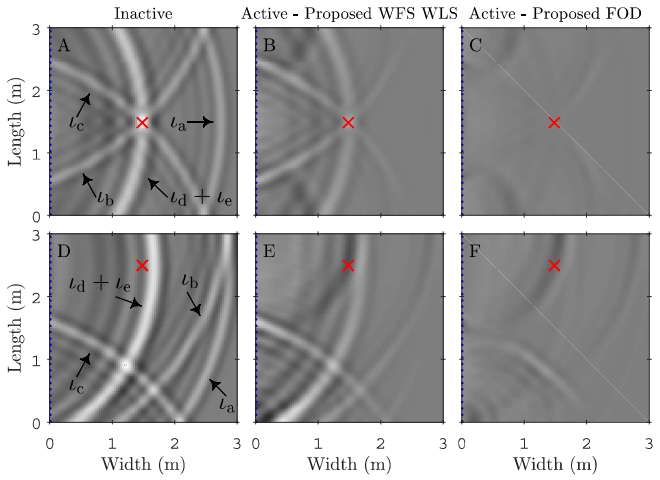

Fig. 3: The time-domain suppression of first and second order reflections that rebound from $\mathcal{C}$ are shown. The red cross marks the location of the primary source (Top row: room centre. Bottom row: $(1.5\,\text{m}, 2.5\,\text{m}, 1.5\,\text{m})$) and amplitudes are grey-scale normalised.

initial investigation of spatial disparities (methods are independent of order) and the image source method is used for evaluation [31], [32].

The WLS frequency response and impulse response can be seen in Fig. 2. The magnitude and phase response are within ± 1 dB and $\pm 1^\circ$ of the desired, respectively. The filter latency is considered neglible at less than 100 µs and is desirable for real-time cancellation.

6.2. Time-Domain Suppression Comparison

The time-domain suppression of a band-limited (150 Hz to 1500 Hz $\ll k_u$) impulse response over a slice of the room ($(x, y, 1.5\,\text{m})$) is shown in Fig. 3 for a primary point source located in the centre of the room (top row) and at $(1.5\,\text{m}, 2.5\,\text{m}, 1.5\,\text{m})$ (bottom row). The labels in (A) and (D) of Fig. 3 are simplified from Fig. 1 with $\iota_a = \iota^{(1)}_{-1,0,0}$, $\iota_b = \iota^{(2)}_{-1,1,0}$, $\iota_c = \iota^{(2)}_{-1,-1,0}$, $\iota_d = \iota^{(2)}_{-1,0,1}$, $\iota_e = \iota^{(2)}_{-1,0,-1}$. Only the reflections that can be suppressed are shown. It is clear from Fig. 3 (B) that suppression of ι_a is greatest due to $H(e^{ik})$ being a better approximation to $F(e^{ik})$ for propagation parallel to $\mathbf{n}$. Fig. 3 (C) shows significant improvement for reflections arriving closer to perpendicular to $\mathbf{n}$ which is a direct result of using higher order models to determine the gradient of the sound field at $\mathcal{C}$.

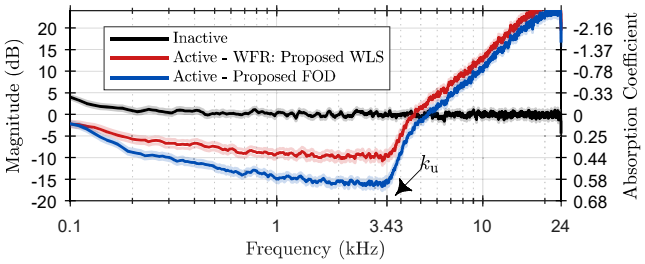

Fig. 4: The mean frequency-domain suppression of all first and second order reflections that rebound from $\mathcal{C}$ is given for the WFR WLS and FOD methods. 95 % confidence intervals are given.

After moving the primary source and observing Fig. 3 (E) it is clear that suppression using the WLS pre-filter works best in the direction of $\mathbf{n}$. Using the FOD models, again, provides a better suppression of reflections arriving from angles off the normal direction, $\mathbf{n}$. The small errors that can be seen in Fig. 3 (C) and (F) are due to the finite length of the arrays and the finite spacings between array elements which cause diffraction at the edges and time-aliased artefacts, respectively, in the recording and reproduction.

6.3. Frequency-Domain Suppression Comparison

The mean frequency suppression and confidence intervals shown in Fig. 4 are computed over 200 randomly positioned primary point sources and observation points. The degradation in performance due to spatial aliasing artefacts above k_u can be seen in Fig. 4 above 3.43 kHz. A cascaded low-latency low-pass filter could be used to mitigate the effect of the spatial aliasing artefacts. While the spatial aliasing artefacts are a limitation of the separation between microphones and loudspeakers, the performance below k_u is significantly better than an inactive system, however, low frequency performance is limited by the finite size of the array. Absorption coefficients [33] are found from reflection coefficients which are equivalent to the suppression [32]. The mean suppression below k_u is 9.2 dB for the WFR WLS method, equivalent to a mean absorption coefficient of 0.41. Further improvements in suppression are observed when using the FOD method with a mean suppression of approximately 14.8 dB below k_u, equivalent to a mean absorption coefficient of 0.57.

7. CONCLUSIONS

We have considered two sound field control techniques for suppressing reflections in closed rooms. We have shown that WFS and WFR systems can be extended to allow real-time low-latency active room compensation using the proposed WLS pre-filter. A system comprised of FOD models has been proposed as an alternative to the WLS pre-filter method and does not assume knowledge of room geometry or primary sources. Comparison of the two proposed methods shows the relative active absorption performance with the WLS pre-filter method providing a mean suppression of 9.2 dB (0.41 absorption coefficient) and the FOD model method providing 14.8 dB of suppression (0.57 absorption coefficient). Future work could look at reducing measures of reverberation, such as RT60, using multiple active walls in different shaped rooms. Predicting wave propagation in rooms using autoregressive models is also a topic for future work.

8. REFERENCES

[1] S. Spors *et al.*, "Spatial sound with loudspeakers and its perception: A review of the current state," *Proc. IEEE*, vol. 101, no. 9, pp. 1920–1938, 2013.

[2] W. Zhang *et al.*, "Surround by Sound: A Review of Spatial Audio Recording and Reproduction," *Appl. Sciences*, vol. 7, no. 6, p. 532, May 2017, doi: 10.3390/app7050532.

[3] Y. Kajikawa *et al.*, "Recent advances on active noise control: Open issues and innovative applications," *APSIPA Trans. Signal Inform. Process.*, vol. 1, pp. 1–21, 2012.

[4] M. A. Poletti, "Active acoustic systems for the control of room acoustics," *Noise & Vibration Worldwide*, vol. 44, no. 4, pp. 10–26, 2013.

[5] D. S. Talagala *et al.*, "Efficient multi-channel adaptive room compensation for spatial soundfield reproduction using a modal decomposition," *IEEE Trans. Audio, Speech, Lang. Process.*, vol. 22, no. 10, pp. 1522–1532, Oct. 2014.

[6] C. Hofmann *et al.*, "Higher-order listening room compensation with additive compensation signals," in *Int. Conf. Acoust., Speech and Signal Process. (ICASSP)*, IEEE, 2016, pp. 534–538.

[7] J. O. Jungmann *et al.*, "Joint time-domain reshaping and frequency-domain equalization of room impulse responses," in *Int. Conf. Acoust., Speech and Signal Process. (ICASSP)*, IEEE, 2014, pp. 6642–6646.

[8] L. Krishnan *et al.*, "A robust sparse approach to acoustic impulse response shaping," in *Int. Conf. Acoust., Speech and Signal Process. (ICASSP)*, IEEE, 2015, pp. 738–742.

[9] K. Kinoshita *et al.*, "A summary of the REVERB challenge: State-of-the-art and remaining challenges in reverberant speech processing research," *EURASIP J. Advances Signal Process.*, vol. 2016, no. 1, Dec. 2016.

[10] S. Spors *et al.*, "Active listening room compensation for massive multichannel sound reproduction systems using wave-domain adaptive filtering," *J. Acoust. Soc. Am.*, vol. 122, no. 1, pp. 354–369, 2007.

[11] S. Spors and H. Buchner, "An approach to massive multichannel broadband feedforward active noise control using wave-domain adaptive filtering," in *Workshop Applicat. Signal Process. Audio Acoust. (WASPAA)*, IEEE, 2007, pp. 171–174.

[12] M. A. Poletti *et al.*, "Higher order loudspeakers for improved surround sound reproduction in rooms," in *Audio Eng. Soc. Conv. 133*, Audio Eng. Soc., 2012.

[13] P. N. Samarasinghe *et al.*, "3D soundfield reproduction using higher order loudspeakers," in *Int. Conf. Acoust., Speech and Signal Process. (ICASSP)*, IEEE, 2013, pp. 306–310.

[14] T. Betlehem and M. A. Poletti, "Two dimensional sound field reproduction using higher order sources to exploit room reflections," *J. Acoust. Soc. Am.*, vol. 135, no. 4, pp. 1820–1833, 2014.

[15] E. G. Williams, *Fourier Acoustics: Sound Radiation and Nearfield Acoustical Holography*. Academic Press, 1999.

[16] J. Ahrens and S. Spors, "Sound field reproduction using planar and linear arrays of loudspeakers," *IEEE Trans. Audio, Speech, Lang. Process.*, vol. 18, no. 8, pp. 2038–2050, 2010.

[17] J. Donley *et al.*, "Active speech control using wave-domain processing with a linear wall of dipole secondary sources," in *Int. Conf. Acoust., Speech and Signal Process. (ICASSP)*, IEEE, 2017, pp. 1–5.

[18] G. N. Lilis *et al.*, "Sound field reproduction using the lasso," *IEEE Trans. Audio, Speech, Lang. Process.*, vol. 18, no. 8, pp. 1902–1912, Nov. 2010.

[19] T. Betlehem and C. Withers, "Sound field reproduction with energy constraint on loudspeaker weights," *IEEE Trans. Audio, Speech, Lang. Process.*, vol. 20, no. 8, pp. 2388–2392, Oct. 2012.

[20] C. Hansen *et al.*, *Active Control of Noise and Vibration, Second Edition*. CRC Press, 2012.

[21] D. Zhou and V. DeBrunner, "A new active noise control algorithm that requires no secondary path identification based on the SPR property," *IEEE Trans. Signal Process.*, vol. 55, no. 5, pp. 1719–1729, May 2007.

[22] M. Wu *et al.*, "An improved active noise control algorithm without secondary path identification based on the frequency-domain subband architecture," *IEEE Trans. Audio, Speech, Lang. Process.*, vol. 16, no. 8, pp. 1409–1419, Nov. 2008.

[23] M. Gao *et al.*, "A simplified subband ANC algorithm without secondary path modeling," *IEEE/ACM Trans. Audio, Speech, Lang. Process.*, vol. 24, no. 7, pp. 1164–1174, Jul. 2016.

[24] P. Zech *et al.*, "Direct adaptive feedforward compensation of narrowband disturbances without explicit identification of the secondary path model," *J. of Sound and Vibration*, vol. 401, pp. 282–296, Aug. 2017.

[25] J. Tao *et al.*, "Performance of a multichannel active sound radiation control system near a reflecting surface," *Appl. Acoust.*, vol. 123, pp. 1–8, Aug. 2017.

[26] J. Cheer and S. J. Elliott, "The design and performance of feedback controllers for the attenuation of road noise in vehicles," *Int. J. Acoust. Vibration*, vol. 19, no. 3, pp. 155–164, 2014.

[27] P. N. Samarasinghe *et al.*, "Recent advances in active noise control inside automobile cabins: Toward quieter cars," *IEEE Signal Process. Mag.*, vol. 33, no. 6, pp. 61–73, Nov. 2016, doi: 10.1109/MSP.2016.2601942.

[28] S. Spors *et al.*, "The theory of wave field synthesis revisited," in *Audio Eng. Soc. Conv. 124*, Audio Eng. Soc., 2008, pp. 17–20.

[29] S. Koyama *et al.*, "Analytical approach to wave field reconstruction filtering in spatio-temporal frequency domain," *IEEE Trans. Audio, Speech, Lang. Process.*, vol. 21, no. 4, pp. 685–696, Apr. 2013.

[30] S. Koyama *et al.*, "Real-time sound field transmission system by using wave field reconstruction filter and its evaluation," *IEICE Trans. on Fundamentals of Electron., Commun. and Comput. Sci.*, vol. 97, no. 9, pp. 1840–1848, 2014.

[31] J. B. Allen and D. A. Berkley, "Image method for efficiently simulating small-room acoustics," *J. Acoust. Soc. of Am.*, vol. 65, pp. 943–950, 1979.

[32] E. A. Habets, "Room impulse response generator," *Technische Universiteit Eindhoven, Tech. Rep*, vol. 2, no. 2, p. 1, 2006.

[33] C.-N. Wang and J.-H. Torng, "Experimental study of the absorption characteristics of some porous fibrous materials," *Appl. Acoust.*, vol. 62, no. 4, pp. 447–459, 2001.